Congresso de Métodos Numéricos em Engenharia 2015
Lisboa, 29 de Junho a 2 de Julho 2015

LINEAR VS NON-LINEAR AEROELASTIC ANALYSIS OF HIGH ASPECT-RATIO WINGS

Frederico Afonso[1], Gonçalo Leal[1], José Vale[1], Éder Oliveira[1], Fernando Lau[1] and Afzal Suleman[1]

1: CCTAE, IDMEC
Instituto Superior Técnico
Universidade de Lisboa
Av. Rovisco Pais, No. 1, 1049-001, Lisboa, Portugal

Keywords: High Aspect-Ratio Wings, Non-linear Aeroelasticity, Fluid-Structure Interaction

Abstract. *A current trend in the aeronautic industry is the increase of wing aspect-ratio to enhance aerodynamic efficiency by reducing the induced drag and thus designing a greener aircraft. Despite the associated benefits of increasing the wing's aspect-ratio, such as higher lift-to-drag ratios and ranges, the commercial jets usually have relatively low aspect-ratios. This is mainly explained by the fact that the wing becomes more flexible by increasing the aspect-ratio and thus more prone to high deflections which can cause aeroelastic instability problems such as, e.g., flutter. The aerospace group at Instituto Superior Técnico is developing a Fluid-Structure Interaction (FSI) software able to analyse wings with high aspect-ratio. For this work, a very simple rectangular wing model is employed, with a NACA0012 aerofoil. Different aspect-ratio wings are analysed with linear and non-linear static aeroelastic solvers. In the end, the flutter speed boundary is assessed for each aspect-ratio wing analysed at the linear or non-linear equilibrium deformed state. Comparisons will be performed between linear and non-linear displacements, natural frequencies and flutter boundary.*

1 INTRODUCTION

The aeronautic industry is searching for *greener* aircraft designs that not only reduce the environmental impact but also allow to increase speed and capacity to face the demand. Several different concepts were and are being proposed to tackle these contradictory requirements. One of the approaches most in vogue is to increase the wing aspect-ratio to improve the aerodynamic efficiency. Wing designs with higher aspect-ratios provide higher lift-to-drag ratios and longer ranges [1].
Despite such performance improvement being known since many years, current commercial aircraft usually present wings with relatively low aspect-ratio. The main reason for

this fact is related to the large deformations at normal operating conditions, associated to the increased flexibility of the wing structure, which originate a geometrical non-linear behaviour and may cause aeroelastic problems [2]. Large wing deformations may change the dynamic behaviour of the wing structure and thus the aeroelastic behaviour of the wing [3]. Hence the importance of evaluating the influence of non-linearities on the aeroelastic behaviour, namely in terms of flutter phenomenon.
Several numerical works have been performed over the past few decades using low fidelity models for the non-linear aeroelastic analyses of high aspect-ratio wings [4-8]. However, only a few experimental studies are available [5,9]. These are based on simple planar straight wing models at low subsonic speeds, with highly flexible structures planned to deformed considerably [10].
This work aims to evaluate the difference between conducting linear and non-linear aeroelastic static analyses on high aspect-ratio wings. For this purpose few metrics were selected and used to compare linear and non-linear analyses: displacements, natural frequencies and flutter boundary.

2 DEVELOPED FRAMEWORK

A computational framework is currently being developed to perform linear and non-linear aeroelastic analyses using a fluid-structure interaction algorithm. This framework was originally developed for preliminary aircraft design in the scope of EU 7th Framework Program Project NOVEMOR. The tool includes the main aircraft disciplines, although for the studies performed in this work only geometric, aerodynamic, structural and fluid-structure interaction modules were employed.
The models are of low/medium fidelity. The aerodynamic model consists in a 3D panel method formulation which accounts for compressibility corrections and estimates the viscous drag for each panel in the model. The structural model is based on a 3D equivalent beam model, which represents the stiffness and mass distributions along the wing span by calculating the inertia properties of the span-wise wing cross-section. Only geometric non-linearities are considered in both structural and aerodynamic models.
The Fluid-Structure Interaction (FSI) module is used to perform all aeroelastic static calculations. This module calculates the linear or non-linear static equilibrium using a monolithic methodology. It coordinates the aerodynamic and structural modules in the sense that it transfers the loads from the aerodynamic panels to the structure and transfers the structural displacements to the aerodynamic panels.
The flutter boundary is computed at the aeroelastic equilibrium state using the p-k method. If a non-linear aeroelastic analysis is conducted, the updated stiffness and mass matrices are used; otherwise the flutter speed calculation is performed using the undeformed stiffness and mass matrices together with the Generalized Aerodynamics Matrix affected by the displaced geometry. The flutter speed is calculated in MSC.NASTRAN^{TM}.

3 WING MODEL

In order to study the effects of increasing wing aspect-ratio in flutter speed, a very simple wing model is employed. This model (Figure 1) consists of a rectangular cantilever wing made of aluminium (properties in Table 1) with a constant wing span of 20 m and a variable chord. The wing aerofoil is a NACA0012.

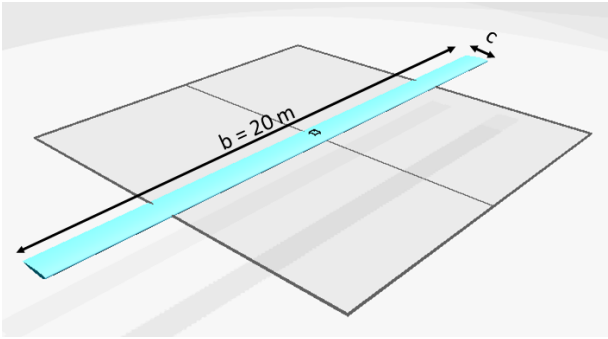

Figure 1: Basic wing model configuration.

Three different high aspect-ratio wings were considered: 20; 24; and 28. The aspect-ratio of the wing is changed by reducing the wing chord (starting with a chord of 1 meter) while at the same time maintaining the wing span and the inertia ratio (I_2/I_1) constant. Consequently the bending and torsional stiffnesses as well as the mass are reduced as the wing chord decreases; thus the displacements for the same flight condition (speed, altitude and angle of attack) are predicted to be higher. The main characteristics of the 3 different wing aspect-ratio configurations are summarized in Table 2.

Table 1: Isotropic aluminium properties.

Parameter	Notation	Value	Unit
Young Modulus	E	70	GPa
Rigidity Modulus	G	27	GPa
Poisson Ratio	ν	0.33	
Density	ρ	2700	kg/m^3

The same flight condition was assumed for all the cases: constant flow speed of 40 [m/s]; sea level altitude conditions; and angle of attack ranging from -4° to 10°. Since non-linear viscous effects and shock waves are not considered in the aerodynamic model, a low subsonic speed was chosen.

Table 2: Main characteristics of the 3 different wing aspect-ratio configurations.

AR [-]	Span [m]	Chord [m]	Area [m^2]	I_2/I_1 [-]	GJ [$N.m^2$]	Mass [kg]
20	20	1.00	20.00	27.12	4.62×10^5	244.56
24	20	0.83	16.67	27.12	2.23×10^5	169.83
28	20	0.71	14.29	27.12	1.20×10^5	124.78

4 RESULTS

All the aeroelastic equilibrium states (linear and non-linear) were computed by using the FSI module. In order to compare both linear and non-linear Fluid-Structure Interaction analyses, the following metrics are investigated: lift coefficient; vertical tip displacement; span-wise twist (incidence angle) distribution; span-wise lift distribution; deformed wing shape; and flutter speed.

In Figure 2 it is noticeable that non-linear effects become more evident when the wing aspect-ratio increases for the same flight conditions (speed, altitude and angle of attack). This fact is not caused by the increase of the aspect-ratio per se, but it is rather caused by the associated reductions of wing mass and both bending and torsional stiffnesses which make the wing more flexible.

Upon looking at Figures 2 (a-c), which show the variation of the lift coefficient (C_L) with the angle of attack (α) for the 3 aspect-ratio wings, one can observe a deviation of C_L from linear variation (with α); that deviation increases noticeably if we turn from linear to non-linear equilibrium states. As a consequence of weakening the wing structure (reduction of the torsional and bending stiffnesses) for the same flight condition (speed, altitude and angle of attack), the displacements are higher (vertical and twist/incidence angle, as can be seen in Figures 2 (d-i)). This changes the lift distribution, as illustrated in Figures 3 (a-c). This effect is observable even if the linear FSI solver (green line with green circles) is used. However, with the non-linear FSI solver (blue line with blue squares) this effect becomes more evident and the deviation from the linear aeroelastic equilibrium state increases as aspect-ratio increases.

The change of the span-wise dimensionless lift distribution with the aspect-ratio caused by the significant wing deformations is shown in Figures 3 (a-c) for the 10° angle of attack case (where the wings suffer higher deformations). The modification of the span-wise lift distribution is due to the increase on bending rotation of the wing (θ_X) (see Figures 3 (d-f)) and the change in the incidence of the aerofoils (see Figures 3 (g-i)) producing the observed different lift distribution. This change is very perceptible even for the linear FSI (green line with green circles). The difference between the linear and non-linear span-wise dimensionless lift distribution becomes more evident as the displacement increases. This difference is caused mainly by the variation of the span-wise distribution of the angle of incidence (very clear in Figure 3 (g-i)) and in a smaller scale by the artificial stretching effect on the span, given by the linear solution (visible on Figures 3 (d-f)).

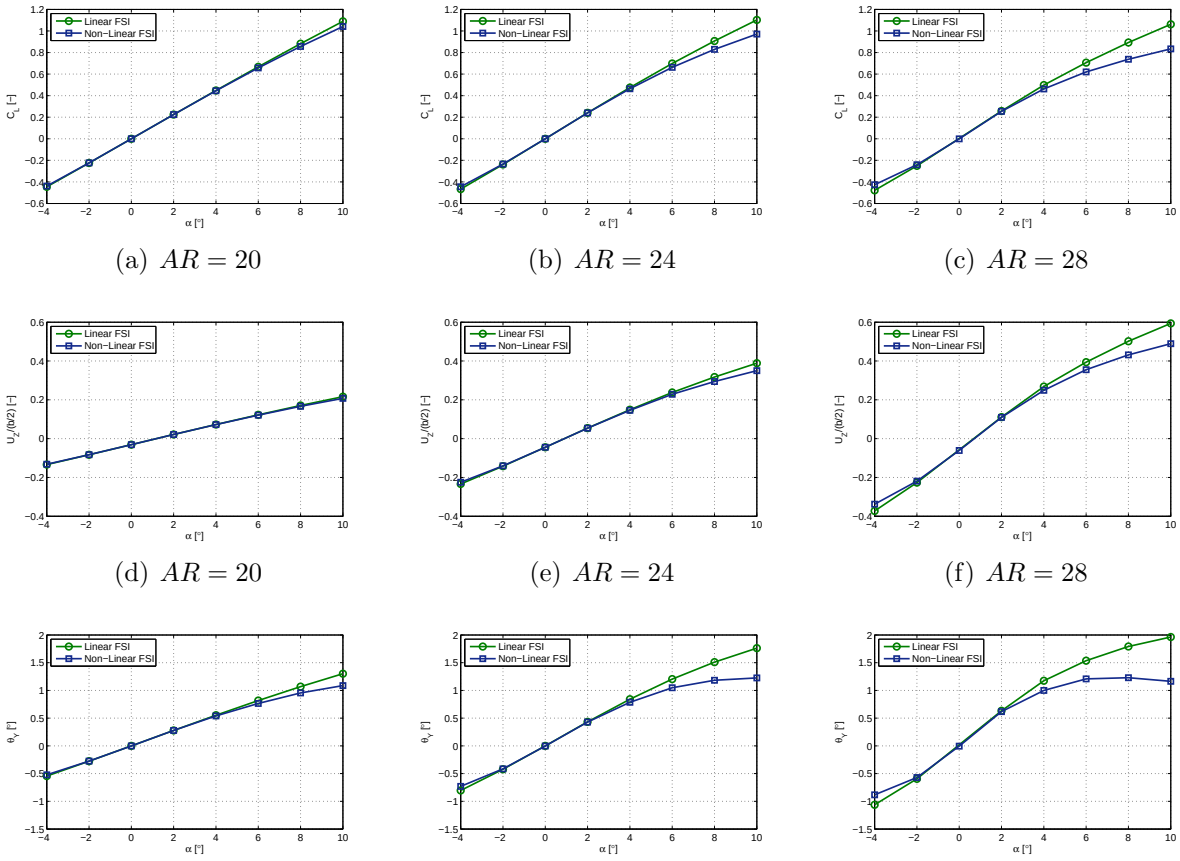

(a) $AR = 20$ (b) $AR = 24$ (c) $AR = 28$

(d) $AR = 20$ (e) $AR = 24$ (f) $AR = 28$

(g) $AR = 20$ (h) $AR = 24$ (i) $AR = 28$

Figure 2: Lift coefficient (top row), dimensionless tip displacement (middle row) and tip twist angle (bottom row) variations with Angle of Attack (α) and Aspect Ratio (AR).

The differences between linear and non-linear aeroelastic equilibrium solutions for the deformed wing shape are not as evident as in the previous observations. Even for the 10° of angle of attack case depicted in Figures 3 (d-f), the linear deformed curve of the wing lies on the non-linear deformed curve, and the stretching effect on the wing tip is the only perceptible difference in the wing deformed shape.

The mode that causes flutter is the first torsion mode for all the aspect-ratio wings, except for the lower tip displacement points (low wing loadings), for which the mode causing flutter is the first edgewise bending mode. In this case, the edgewise bending mode is damped as deformation increases.

The discrepancy between linear and non-linear FSI solutions is quite noticeable in the flutter speed plots (Figures 4 (d-f)), in which even for a stiffer wing ($AR = 20$) one can observe these differences. Since the linear aeroelastic equilibrium solution of the wing presents higher displacements (vertical tip displacement and tip twist angle), the loading is higher and thus the flutter speed is lower when compared with the non-linear solutions.

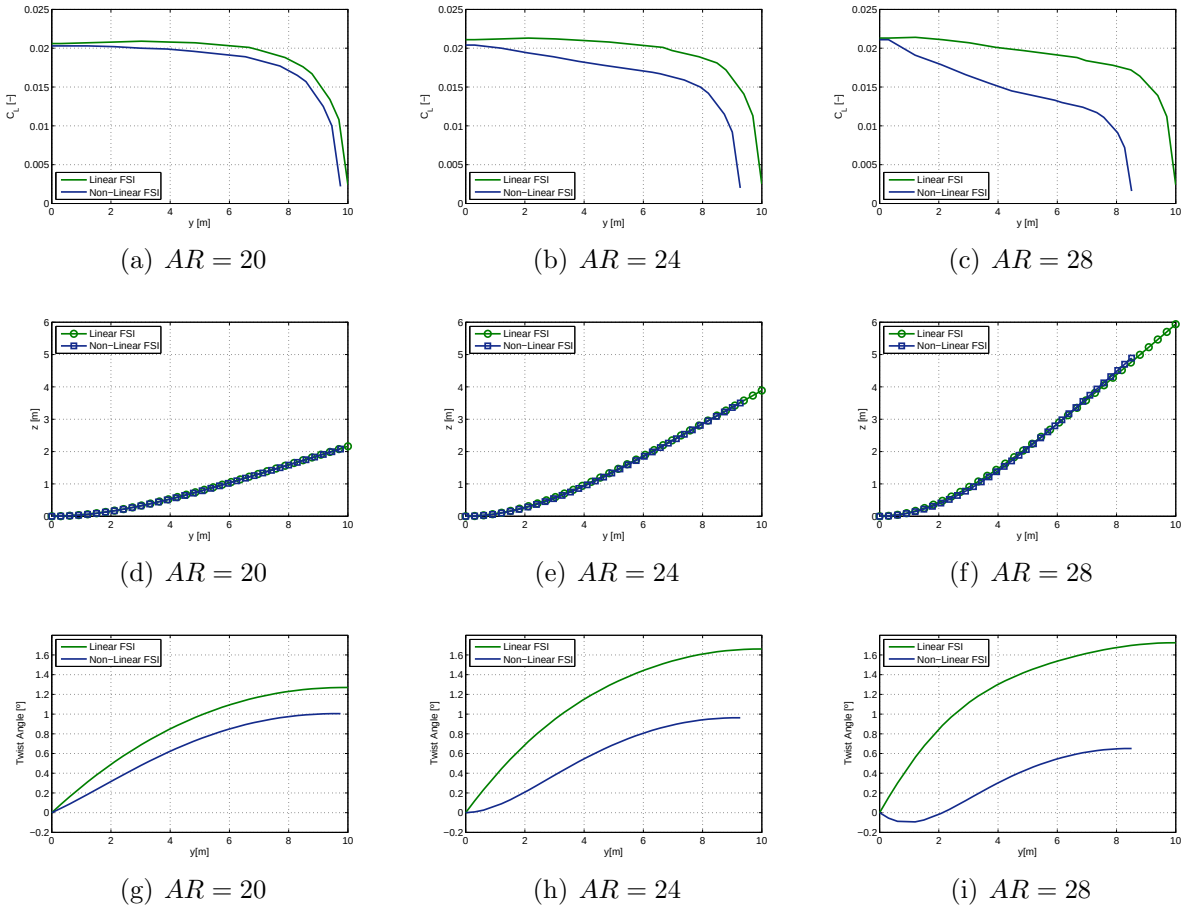

(a) $AR = 20$ (b) $AR = 24$ (c) $AR = 28$

(d) $AR = 20$ (e) $AR = 24$ (f) $AR = 28$

(g) $AR = 20$ (h) $AR = 24$ (i) $AR = 28$

Figure 3: Span-wise lift coefficient distribution (top row), wing deformed shape (center row) and span-wise incidence angle distribution (bottom row) variations with the aspect-ratio (AR).

Hence the importance of taking the deformed state into account when computing the flutter speed. For high angle of attack conditions, the higher displacements obtained for the wing with higher aspect-ratio cause an inflexion on the trend of flutter speed increase with tip displacement; this is caused by the variation on span-wise incidence angle distribution with the angle of attack, as shown in Figures 4 (a-c): this parameter has a particular high influence on the torsional mode shape and consequently on the flutter speed. For the lower aspect-ratio wing ($AR = 20$), no inflexion on span-wise incidence angle distribution is observed, although for the higher aspect-ratio wings this behaviour was found for the higher angles of attack.

If one plots the flutter speed difference (between the linear and non-linear solutions) as a function of the vertical tip displacement difference (between the linear and non-linear solutions) one can find in Figure 5 that regardless of the wing aspect-ratio and the magnitude of the displacement, there is a linear dependence between those two factors. A very small difference between slopes is observable in Figure 5 for the 3 aspect-ratio

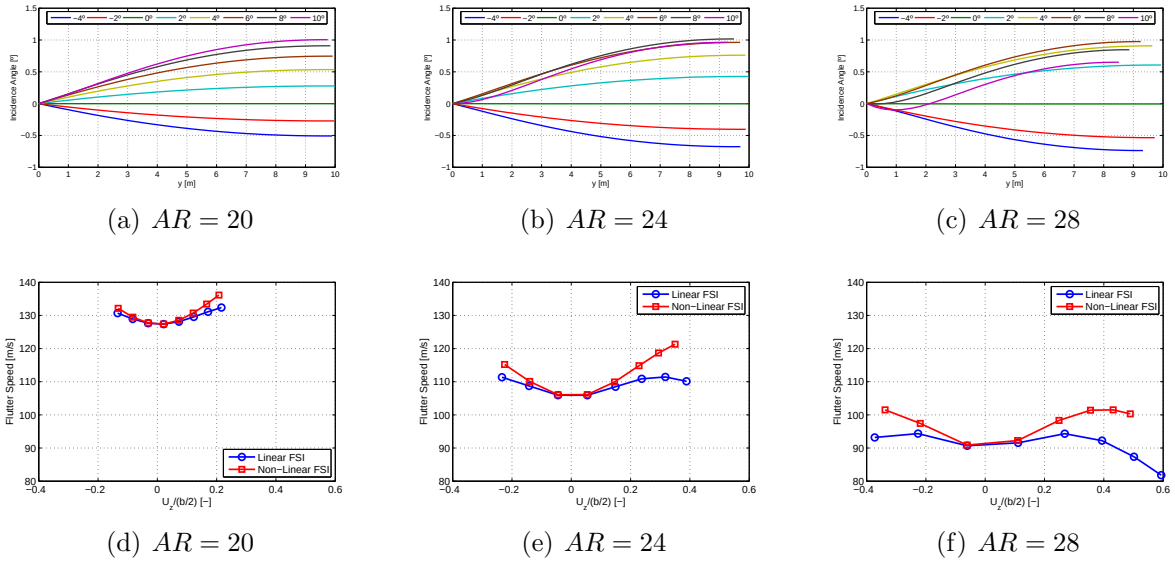

(a) $AR = 20$ (b) $AR = 24$ (c) $AR = 28$

(d) $AR = 20$ (e) $AR = 24$ (f) $AR = 28$

Figure 4: Span-wise incidence angle distribution for different angles of attack (α) (top row) and flutter speed in function of dimensionless tip displacement (bottom row) variations with Aspect Ratio (AR).

wings. From Figure 5 one can also observe that the flutter speed difference increases as the vertical tip displacement difference increases.

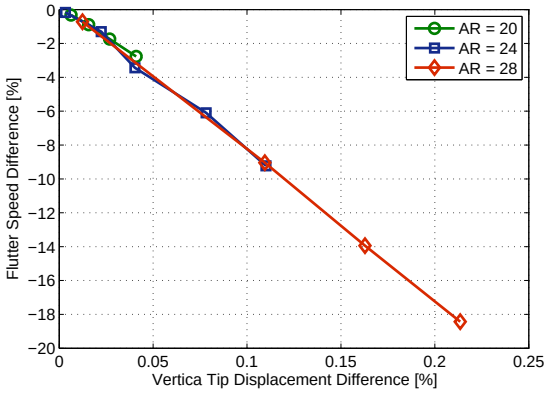

Figure 5: Flutter speed difference (relative difference between linear and non-linear) in function of vertical tip displacement difference (relative difference between linear and non-linear).

5 CONCLUSIONS

Significant differences between linear and non-linear aeroelastic equilibrium solutions were found in this study. These differences were observed to increase as the wing aspect-ratio increases. However, the main cause of this behaviour is not the increase on wing aspect-ratio per se, but rather the reduction on wing mass, torsional stiffness and bending stiffness

which weakened the wing, rendering it more flexible and prone to higher deformation. The increase on deformation makes the differences in the deformed state from linear to non-linear solutions more evident (mainly due to the variation on twist/incidence angle span-wise distribution), in terms of both span-wise dimensionless lift distribution and flutter speed. A linear correlation of flutter difference with vertical tip displacement difference was observed.

ACKNOWLEDGEMENTS

The presented work was carried out as part of the EU FP7 Project NOVEMOR and the authors thank the European Commission for funding this research (Grant Agreement 285395).

REFERENCES

[1] I.H. Abbott and A.E. Von Doenhoff, *Theory of wing sections, including a summary of airfoil data*, Dover Publications, (1959).

[2] J.E. Cooper and M.Y. Harmin, *Dynamic Aeroelastic Prediction For Geometrically Nonlinear Aicraft*, *International Forum on Aeroelasticity and Structural Dynamics (IFASD) 2011*, Paris, France (2011).

[3] M.J. Patil, D.H. Hodges and C.E.S. Cesnik. Nonlinear Aeroelasticity and Flight Dynamics of High-Altitude Long-Endurance Aircraft, *Journal of Aircraft*, Vol. **38**, No. 1, pp. 88–94, (2001).

[4] M.J. Patil, D.H. Hodges and C.E.S. Cesnik, *Characterizing the Effects of Geometrical Nonlinearities on Aeroelastic Behavior of High-Aspect-Ratio Wings*, *International Forum on Aeroelasticity and Structural Dynamics (IFASD) 1999*, Williamsburg, Virginia, USA (1999).

[5] D. Tang and E.H. Dowell. Experimental and theoretical study on aeroelastic response of high-aspect-ratio wings, *AIAA Journal*, Vol. **39**, No. 8, pp. 1430–1441, (2001).

[6] E.H. Dowell and D. Tang. Effects of geometric structural nonlinearity on flutter and limit cycle oscillations of high-aspect-ratio wings, *Journal of Fluid and Structure*, Vol. **19**, pp. 291–306, (2004).

[7] M.J. Patil and D.H. Hodges. On the importance of aerodynamic and structural geometrical nonlinearities in aeroelastic behavior of high-aspect-ratio wing, *Journal of Fluid and Structure*, Vol. **19**, pp. 905–915, (2004).

[8] A. Arena, W. Lacarbonara and P. Marzocca, *Nonlinear aeroelastic formulation for flexible high-aspect ratio wings via geometrically exact approach*, *52nd*

AIAA/ASME/ASCE/AHS/ASC Structures, Structural Dynamics and Materials Conference, Denver, Colorado, USA, (2011).

[9] P. Dunn and J. Dugundji. Nonlinear stall flutter and divergence analysis of cantilevered graphit/epoxy wings, *AIAA Journal* Vol. **30**, No. 1, pp. 153–162, (1992).

[10] M. Kampchen, A. Dafnis, H.G. Reimerdes, G. Britten, J. Ballmann. Dynamic aerostructural response of an elastic wing model, *Journal of Fluid and Structure*, Vol. **18**, pp. 63-77, (2003).